Journal of Quantitative Spectroscopy & Radiative Transfer 131 (2013) 188–193

Contents lists available at ScienceDirect

Journal of Quantitative Spectroscopy & Radiative Transfer

journal homepage: www.elsevier.com/locate/jqsrt

Measuring the void: Theoretical study of scattering by a cylindrical annulus

Alex J. Yuffa *, John A. Scales

Department of Physics, Colorado School of Mines, Golden, CO 80401, USA

ARTICLE INFO

Article history:
Received 30 November 2012
Received in revised form
4 February 2013
Accepted 18 February 2013
Available online 28 February 2013

Keywords:
Scalar waves
Electromagnetic scattering
Lorenz–Mie theory
Energy extinction
Concentric cylinders

ABSTRACT

In this paper, we analyze a monochromatic plane wave scattering from an infinite homogeneous cylindrical annulus. In particular, we study the effect that the inner part of the cylindrical annulus (cylindrical void, if you will) has on the scattered field. This is done by isolating the cylindrical void's contribution to the scattered field. We show that if the cylindrical void is small, then its contribution to the scattered field may be approximated by the "screened cylindrical void" (SCV) approximation. We first develop the SCV approximation in a physically intuitive manner, and then show that it could also be obtained in a more mathematically rigorous manner. Numerical results comparing the SCV approximation to the exact solution are also presented.

1. Introduction

Consider a monochromatic plane wave scattering from an infinitely long homogeneous and isotropic cylindrical annulus with outer radius r_1 and inner radius r_2, see Fig. 1a. Let ϵ_1 denote the permittivity of the space surrounding the cylindrical annulus and let ϵ_2 denote the permittivity of the cylindrical annulus itself, $r_2 < r < r_1$. Let us refer to the region of space inside the cylindrical annulus as the "cylindrical void" and ask what effect the cylindrical void has on the scattered field(s) outside the cylindrical annulus. If one were to *experimentally* investigate this, one would do the following:

(a) measure the total field $V^{(1)}(r,\theta)$ outside the cylindrical annulus ($r > r_1$);
(b) measure the total field $U^{(1)}(r,\theta)$ outside an identical "host cylinder;" i.e., a cylinder of radius r_1 and permittivity ϵ_2, as illustrated in Fig. 1b;
(c) compute the difference between the two fields in (a) and (b):

$$W^{(\mathrm{sca})}(r,\theta) = V^{(1)}(r,\theta) - U^{(1)}(r,\theta). \tag{1}$$

Following the above procedure, $W^{(\mathrm{sca})}(r,\theta)$ contains the effect that the cylindrical void had on the scattered field. In this paper, we show that $W^{(\mathrm{sca})}(r,\theta)$ can be approximated by the scattered field produced by the cylindrical void when a plane wave from a region of space with a permittivity of ϵ_2 is incident on it. This approximation holds if the "screening effect" (discussed in Section 2) of the cylindrical annulus is properly accounted for, and if the cylindrical void is sufficiently small. We refer to this approximation as the *screened cylindrical void* (SCV) approximation. Furthermore, we investigate the rate, denoted by $\mathbb{W}^{\mathrm{ext}}$, at which the energy is extinguished (depleted) by the cylindrical void from the total field outside, $U^{(1)}(r,\theta)$, the host cylinder.

To the best of our knowledge, the SCV approximation and its physical interpretation (see Section 2) has not been

* Corresponding author. Tel.: +1 720 933 0654.
E-mail addresses: ayuffa@gmail.com, ayuffa@mines.edu (A.J. Yuffa).
URL: http://mesoscopic.mines.edu (J.A. Scales).

0022-4073/$ - see front matter © 2013 Elsevier Ltd. All rights reserved.
http://dx.doi.org/10.1016/j.jqsrt.2013.02.017

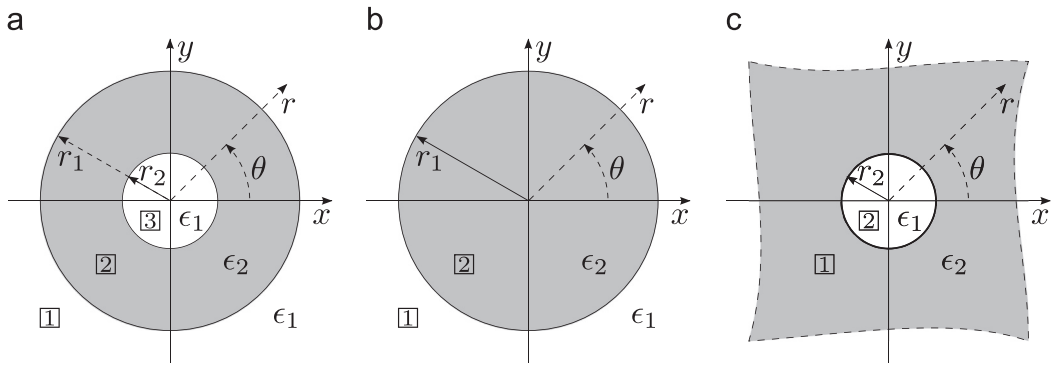

Fig. 1. The cross-sectional view of the cylindrical scattering objects is shown. The origin of the coordinate system (r,θ), where $-\pi \le \theta < \pi$, is concentric with the cylindrical objects. In each panel, the region is denoted by a boxed number and the permittivity of each region is also indicated. For example, region three, $r < r_2$, in panel (a) has a permittivity of ϵ_1 and region one, $r > r_2$, in panel (c) has a permittivity of ϵ_2.

previously considered in the literature. In order to make the paper accessible to the widest possible scientific community, we use the well-known Lorenz–Mie theory [1–4] to derive the SCV approximation. However, we do note that our intuitive derivation of the SCV approximation, which is presented in Section 2, is *physically guided* by the Debye series expansion [5]. In short, the Debye series expansion consists of re-expressing *each* Mie scattering coefficient in terms of an infinite series called the Debye series. Each term in the Debye series may be physically interpreted in terms of the number of reverberations the wave has experienced. A reader interested in the use of the Debye series expansion in the context related to this paper, namely, plane wave scattering by a multilayered cylinder, may consult [6,7] and references therein.

Although we do not explicitly consider many diverse areas of science where the scattering by a cylindrical void is important (e.g., see [3,4]), we would like to mention one, namely, localization. Fifty years after the publication of Anderson's seminal work [8], localization continues to be a thriving area of research [9] in theoretical and experimental physics. Localization of millimeter/submillimeter electromagnetic waves is particularly interesting because both the amplitude and the phase of the electromagnetic field can be easily measured with a vector network analyzer [10]. At these wavelengths, the preparation of disordered samples is also inexpensive and straightforward with standard computer-numerically-controlled (CNC) milling techniques. A sample may be prepared by drilling small holes in a large Teflon (ultra low-loss material) cylinder. Further, by illuminating the sample from the side and putting it on a rotational stage, we can generate essentially arbitrary realizations of the same random disorder. When the number of small scatterers is large, say, over 1000, then what is important is the rate at which the scatterer extinguishes the energy from the incident field, rather than the geometrical shape/size of each individual scatterer [11,12]. Thus, the physical insight into scattering by a single small cylindrical void discussed in this paper may be of benefit in understanding the experimental model described above.

Throughout this paper, we will use the Gaussian unit system, and we will assume that all fields are harmonic in time with a $\exp(-i\omega t)$ time factor, where ω is the angular frequency. Furthermore, we will assume that all fields are polarized in the positive $\hat{\mathbf{z}}$-direction. The positive $\hat{\mathbf{z}}$-direction is out of the page in Fig. 1. All media considered in this paper are assumed to be non-magnetic, and ϵ_1 is assumed to be purely real.

2. Intuitive derivation of the SCV approximation

In this section, a physically intuitive derivation of the SCV approximation is presented. The derivation is organized as follows. First, we imagine a unit plane wave $u^{(\mathrm{inc})}(r,\theta)$ incident from region one onto the cylindrical void shown in Fig. 1c. Then, we compute the scattered field $u^{(\mathrm{sca})}(r,\theta)$ in region one generated by the scattering of $u^{(\mathrm{inc})}(r,\theta)$ from the cylindrical void. Second, to account for the screening effect of the cylindrical annulus, we use the previously found scattered field $u^{(\mathrm{sca})}(r,\theta)$ as the *incident* (primary) field, i.e., $w^{(\mathrm{inc})}(r,\theta) \equiv u^{(\mathrm{sca})}(r,\theta)$, originating from the center of the host cylinder shown in Fig. 1b. Finally, we compute the total field $w^{(1)}(r,\theta)$ in region one shown in Fig. 1b and physically interpret the terms contained in it to obtain an approximation to $W^{(\mathrm{sca})}(r,\theta)$, see (1).

Let us note that all fields in this paper satisfy the two-dimensional (2D) Helmholtz equation. The radial solution of the 2D Helmholtz equation is composed of a linear combination of integer order Bessel functions of the first and second kind, which we denote by $J_n(\xi)$ and $Y_n(\xi)$, respectively. The Bessel functions $J_n(\xi)$ and $Y_n(\xi)$ also satisfy the Wronskian relationship [13], namely

$$J_{n+1}(\xi)Y_n(\xi) - J_n(\xi)Y_{n+1}(\xi) = \frac{2}{\pi\xi}. \tag{2a}$$

Also, $J_n(\xi)$, $Y_n(\xi)$ and the Hankel function of the first kind, which we denote by $H_n(\xi) = J_n(\xi) + iY_n(\xi)$, satisfy the recurrence relation [13]

$$\frac{d}{d\xi}\Psi_n(\xi) = \frac{n}{\xi}\Psi_n(\xi) - \Psi_{n+1}(\xi), \tag{2b}$$

where Ψ denotes J, Y or H. Lastly, we note the Jacobi–Anger expansion of a plane wave [13], namely,

$$e^{i\xi\cos\theta} = \sum_{n=0}^{\infty} g_n i^n J_n(\xi)\cos(n\theta), \tag{2c}$$

where g_n denotes the Neumann factor: $g_0 = 1$ and $g_n = 2$ for $n \geq 1$.

Returning to the scattering of the unit plane wave from the cylindrical void shown in Fig. 1c, let the incident wave be $u^{(\mathrm{inc})}(r,\theta) = \exp(\mathrm{i}k_2 r\cos\theta)$, where $k_2 = \sqrt{\epsilon_2}\omega/c$ is the wavenumber and c is the speed of light in a vacuum. Then, the field in region two $u^{(2)}(r,\theta)$, and the total field in region one decomposed as $u^{(1)}(r,\theta) = u^{(\mathrm{inc})}(r,\theta) + u^{(\mathrm{sca})}(r,\theta)$, may be written as

$$\begin{bmatrix} u^{(\mathrm{inc})}(r,\theta) \\ u^{(\mathrm{sca})}(r,\theta) \\ u^{(2)}(r,\theta) \end{bmatrix} = \sum_{n=0}^{\infty} g_n \mathrm{i}^n \begin{bmatrix} J_n(k_2 r) \\ \delta_n H_n(k_2 r) \\ \gamma_n J_n(k_1 r) \end{bmatrix} \cos(n\theta), \tag{3}$$

where $k_1 = \sqrt{\epsilon_1}\omega/c$. In writing (3), we used the Jacobi–Anger expansion (2c) to rewrite $\exp(\mathrm{i}k_2 r\cos\theta)$ as an infinite sum, imposed the Sommerfeld radiation (*outgoing* cylindrical wave) condition on $u^{(\mathrm{sca})}(r,\theta)$, and required $u^{(2)}(r,\theta)$ to be regular (finite) at $r=0$. To find the unknown coefficients in (3), we require that the electric field and its normal derivative be continuous across the $r = r_2$ interface, i.e.,

$$u^{(1)} = u^{(2)} \quad \text{and} \quad \frac{\partial}{\partial r}u^{(1)} = \frac{\partial}{\partial r}u^{(2)} \quad \text{on } r = r_2, \tag{4}$$

to obtain a system of linear equations. Solving this system of linear equations for δ_n and using (2b) to simplify the result, yields

$$\delta_n = -\frac{J_{n+1}(k_1 r_2)J_n(k_2 r_2) - \kappa J_n(k_1 r_2)J_{n+1}(k_2 r_2)}{J_{n+1}(k_1 r_2)H_n(k_2 r_2) - \kappa J_n(k_1 r_2)H_{n+1}(k_2 r_2)}, \tag{5a}$$

where $\kappa = k_2/k_1$, $n \in \mathbb{Z}^+$ and $\mathbb{Z}^+$ denotes the set of all nonnegative integers. It is convenient to introduce curly bracket notation, $\{\Psi_{n+1}(\xi), \Phi(\eta)\}$, by which we mean

$$\{\Psi_{n+1}(\xi), \Phi_n(\eta)\} \equiv (\Psi_{n+1}(\xi)\Phi_n(\eta) - \kappa\Psi_n(\xi)\Phi_{n+1}(\eta)).$$

For example, (5a) in the curly bracket notation reads as

$$\delta_n = -\frac{\{J_{n+1}(k_1 r_2), J_n(k_2 r_2)\}}{\{J_{n+1}(k_1 r_2), H_n(k_2 r_2)\}}, \quad n \in \mathbb{Z}^+. \tag{5b}$$

Having found the expansion coefficients of the scattered wave $u^{(\mathrm{sca})}(r,\theta)$, we are now ready to see how they should be modified in order to account for the screening effect of the cylindrical annulus.

Imagine a "line-source" embedded in the center of the host cylinder shown in Fig. 1b. We take the field produced by the line-source to be equal to $u^{(\mathrm{sca})}(r,\theta)$ in (3). If we use this field as the incident field, i.e., $w^{(\mathrm{inc})}(r,\theta) \equiv u^{(\mathrm{sca})}(r,\theta)$, then the total field $w^{(2)}(r,\theta)$ *inside* the host cylinder (region two in Fig. 1b) may be written as $w^{(2)}(r,\theta) = w^{(\mathrm{inc})}(r,\theta) + w^{(\mathrm{sca})}(r,\theta)$, where

$$w^{(\mathrm{sca})}(r,\theta) = \sum_{n=0}^{\infty} g_n \mathrm{i}^n \beta_n J_n(k_2 r)\cos(n\theta). \tag{6a}$$

Notice that in (6a), we required $w^{(\mathrm{sca})}(r,\theta)$ to be regular at $r=0$. This requirement is necessary because we are essentially treating the cylindrical void as a line-source in this paragraph. The field *outside* the host cylinder (region one in Fig. 1b), $w^{(1)}(r,\theta)$, must satisfy the Sommerfeld radiation condition and thus, it is given by

$$w^{(1)}(r,\theta) = \sum_{n=0}^{\infty} g_n \mathrm{i}^n \alpha_n H_n(k_1 r)\cos(n\theta). \tag{6b}$$

Imposing the boundary conditions $w^{(1)} = w^{(2)}$ and $(\partial/\partial r)w^{(1)} = (\partial/\partial r)w^{(2)}$ on $r = r_1$, then solving the resultant linear system for α_n and using (2a) with (2b) to simplify the result yields

$$\alpha_n = \left(\frac{-2\mathrm{i}}{\pi k_1 r_1 \{H_{n+1}(k_1 r_1), J_n(k_2 r_1)\}}\right)\delta_n, \quad n \in \mathbb{Z}^+. \tag{7}$$

We physically interpret the term in parentheses in (7) as the screening effect of the cylindrical annulus on the scattered wave generated by the cylindrical void. The α_n coefficients are not quite the correct ones to use in $W^{(\mathrm{sca})}(r,\theta)$ because they do *not* contain the screening effect that the cylindrical annulus had on the *incident* wave. A moment's thought reveals that this screening effect had to be the same as the screening effect on the scattered wave. Thus, the $W^{(\mathrm{sca})}(r,\theta)$ expansion coefficients should be given by (7) with the parenthesis term *squared*. Therefore, $W^{(\mathrm{sca})}(r,\theta)$ is approximately given by

$$W^{(\mathrm{sca})}(r,\theta) \cong \sum_{n=0}^{\infty} g_n \mathrm{i}^n \left(\frac{-2\mathrm{i}}{\pi k_1 r_1 \{H_{n+1}(k_1 r_1), J_n(k_2 r_1)\}}\right)^2 \times \delta_n H_n(k_1 r)\cos(n\theta), \tag{8}$$

where the δ_n coefficients are given by (5).

3. Rigorous derivation of the SCV approximation

In this section, we present a rigorous derivation of $W^{(\mathrm{sca})}(r,\theta)$ by directly computing $U^{(1)}(r,\theta)$ and $V^{(1)}(r,\theta)$ (recall the bullet list of Section 1). Once the *exact* $W^{(\mathrm{sca})}(r,\theta)$ is found, we show that it is approximately equal to (8) if $k_1 r_2 \ll 1$ and $|k_2| r_2 \ll 1$. Furthermore, a numerical illustration of the SCV approximation is also presented.

If a plane wave, $U^{(\mathrm{inc})}(r,\theta) = \exp(\mathrm{i}k_1 r\cos\theta)$, is incident on the host cylinder shown in Fig. 1b, then by proceeding as in paragraph three of Section 2, the total field in region one is $U^{(1)}(r,\theta) = U^{(\mathrm{inc})}(r,\theta) + U^{(\mathrm{sca})}(r,\theta)$, where the scattered field is

$$U^{(\mathrm{sca})}(r,\theta) = \sum_{n=0}^{\infty} g_n \mathrm{i}^n A_n^{(\mathrm{hc})} H_n(k_1 r)\cos(n\theta) \tag{9a}$$

with

$$A_n^{(\mathrm{hc})} = -\frac{\{J_{n+1}(k_1 r_1), J_n(k_2 r_1)\}}{\{H_{n+1}(k_1 r_1), J_n(k_2 r_1)\}}, \quad n \in \mathbb{Z}^+, \tag{9b}$$

and the field in region two is given by

$$U^{(2)}(r,\theta) = \sum_{n=0}^{\infty} g_n \mathrm{i}^n B_n^{(\mathrm{hc})} J_n(k_2 r)\cos(n\theta). \tag{9c}$$

The superscript (hc) on the expansion coefficients in (9) is meant to remind the reader that these expansion coefficients are for the *h*ost *c*ylinder.

Turning our attention to the cylindrical annulus shown in Fig. 1a, if we think of the cylindrical annulus as the host cylinder into which a scatterer, namely, the cylindrical void, has been inserted, then, the total fields in regions

one, two, and three may be written as $V^{(1)}(r,\theta)=U^{(1)}(r,\theta)+W^{(\mathrm{sca})}(r,\theta)$, $V^{(2)}(r,\theta)=U^{(2)}(r,\theta)+W^{(2)}(r,\theta)$ and $V^{(3)}(r,\theta)=W^{(3)}(r,\theta)$, respectively. Noting that the W-fields also satisfy the 2D Helmholtz equation and imposing the Sommerfeld radiation condition on $W^{(\mathrm{sca})}(r,\theta)$, as well as requiring $W^{(3)}(r,\theta)$ to be regular at $r=0$ yields

$$\begin{bmatrix} W^{(\mathrm{sca})}(r,\theta) \\ W^{(2)}(r,\theta) \\ W^{(3)}(r,\theta) \end{bmatrix} = \sum_{n=0}^{\infty} g_n \mathrm{i}^n \begin{bmatrix} A_n^{(\mathrm{cv})} H_n(k_1 r) \\ B_n^{(\mathrm{cv})} J_n(k_2 r) + C_n^{(\mathrm{cv})} Y_n(k_2 r) \\ D_n^{(\mathrm{cv})} J_n(k_1 r) \end{bmatrix} \cos(n\theta). \tag{10}$$

The superscript (cv) on the expansion coefficients in (10) reminds us of the presence of the *cylindrical void*. To find the unknown coefficients in (10), we require that the V-fields and their normal derivatives be continuous across the $r=r_1$ interface, as well as the $r=r_2$ interface to obtain

$$\underbrace{\begin{bmatrix} -H_n(k_1 r_1) & J_n(k_2 r_1) & Y_n(k_2 r_1) & 0 \\ -H_n'(k_1 r_1) & \kappa J_n'(k_2 r_1) & \kappa Y_n'(k_2 r_1) & 0 \\ 0 & J_n(k_2 r_2) & Y_n(k_2 r_2) & -J_n(k_1 r_2) \\ 0 & \kappa J_n'(k_2 r_2) & \kappa Y_n'(k_2 r_2) & -J_n'(k_1 r_2) \end{bmatrix}}_{=M} \begin{bmatrix} A_n^{(\mathrm{cv})} \\ B_n^{(\mathrm{cv})} \\ C_n^{(\mathrm{cv})} \\ D_n^{(\mathrm{cv})} \end{bmatrix}$$

$$= \begin{bmatrix} J_n(k_1 r_1) + A_n^{(\mathrm{hc})} H_n(k_1 r_1) - B_n^{(\mathrm{hc})} J_n(k_2 r_1) \\ J_n'(k_1 r_1) + A_n^{(\mathrm{hc})} H_n'(k_1 r_1) - \kappa B_n^{(\mathrm{hc})} J_n'(k_2 r_1) \\ -B_n^{(\mathrm{hc})} J_n(k_2 r_2) \\ -\kappa B_n^{(\mathrm{hc})} J_n'(k_2 r_2) \end{bmatrix}, \tag{11}$$

and the prime denotes the derivative with respect to the argument. Solving (11) for $A_n^{(\mathrm{cv})}$ and using (2b) to simplify the result, yields

$$\det(M) A_n^{(\mathrm{cv})} = -\{J_{n+1}(k_1 r_2), J_n(k_2 r_2)\} \times \left(A_n^{(\mathrm{hc})} \{H_{n+1}(k_1 r_1), Y_n(k_2 r_1)\} + \{J_{n+1}(k_1 r_1), Y_n(k_2 r_1)\}\right), \tag{12a}$$

where

$$\det(M) = \{H_{n+1}(k_1 r_1), Y_n(k_2 r_1)\}\{J_{n+1}(k_1 r_2), J_n(k_2 r_2)\} - \{H_{n+1}(k_1 r_1), J_n(k_2 r_1)\}\{J_{n+1}(k_1 r_2), Y_n(k_2 r_2)\}. \tag{12b}$$

To simplify (12a) further, we use (9b) and note that

$$\{Y_{n+1}(k_1 r_1), Y_n(k_2 r_1)\}\{J_{n+1}(k_1 r_1), J_n(k_2 r_1)\} - \{Y_{n+1}(k_1 r_1), J_n(k_2 r_1)\}\{J_{n+1}(k_1 r_1), Y_n(k_2 r_1)\} = \left(\frac{2}{\pi k_1 r_1}\right)^2$$

to obtain

$$A_n^{(\mathrm{cv})} = \frac{\mathrm{i}}{\det(M)} \left(\frac{2}{\pi k_1 r_1}\right)^2 \frac{\{J_{n+1}(k_1 r_2), J_n(k_2 r_2)\}}{\{H_{n+1}(k_1 r_1), J_n(k_2 r_1)\}}, \quad n \in \mathbb{Z}^+. \tag{13}$$

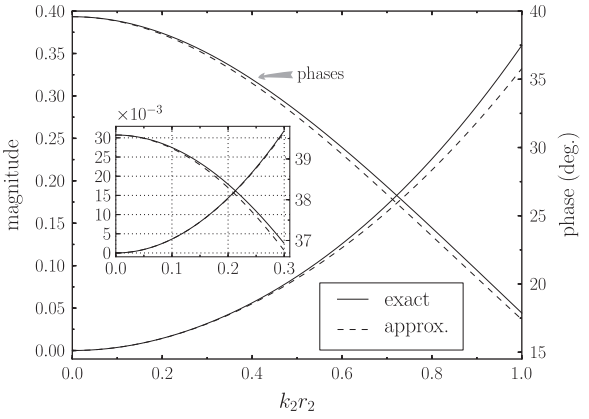

Fig. 2. The magnitude and phase of the far-field pattern in the forward direction for a Teflon cylindrical annulus in vacuum, with an outer radius of 10 cm at 100 GHz, is shown. The permittivity of Teflon at 100 GHz is 2.05 with a negligible loss-tangent [10]. In the computation of (16), we only summed the first $N=\lceil k_1 r_2 + 4(k_1 r_2)^{1/3} + 2 \rceil$ terms [3, Appendix C].

The $A_n^{(\mathrm{cv})}$ coefficients in (13) are the *exact* expansion coefficients of $W^{(\mathrm{sca})}(r,\theta)$. To obtain the approximate coefficients, we first note that $Y_n(k_2 r_2) \sim -\mathrm{i} H_n(k_2 r_2))$ if $|k_2| r_2 \ll 1$ [13], which allows us to rewrite (13) as

$$A_n^{(\mathrm{cv})} \cong \mathrm{i}\left(\frac{2}{\pi k_1 r_1}\right)^2 \frac{1}{\{H_{n+1}(k_1 r_1), J_n(k_2 r_1)\}} \times \left(\frac{\delta_n}{\{H_{n+1}(k_1 r_1), Y_n(k_2 r_1)\}\delta_n - \mathrm{i}\{H_{n+1}(k_1 r_1), J_n(k_2 r_1)\}}\right), \tag{14}$$

where δ_n is given by (5). To develop (14) further, we note that $|\delta_n| \ll 1$ if $k_1 r_2 \ll 1$ and $|k_2| r_2 \ll 1$, as can be seen from the small argument forms of $J_n(\xi)$ and $H_n(\xi)$ [13]. Therefore, we can expand (14) in powers of δ_n to finally obtain

$$A_n^{(\mathrm{cv})} \approx \left(\frac{2\mathrm{i}}{\pi k_1 r_1 \{H_{n+1}(k_1 r_1), J_n(k_2 r_1)\}}\right)^2 \delta_n, \quad n \in \mathbb{Z}^+. \tag{15}$$

Notice that the above $A_n^{(\mathrm{cv})}$ coefficients are identical to the expansion coefficients given in (8) of Section 2.

To numerically illustrate the SCV approximation, the far-field pattern of $W^{(\mathrm{sca})}(r,\theta)$ in the forward direction, $\theta=0$, as a function of $k_2 r_2$ is shown in Fig. 2. The far-field pattern of $W^{(\mathrm{sca})}(r,\theta)$ is defined by

$$F(\theta) = -\sum_{n=0}^{\infty} g_n A_n^{(\mathrm{cv})} \cos(n\theta). \tag{16}$$

From Fig. 2, we see that the exact (computed with (13)) and the approximate (computed with (15)) far-field patterns are in good agreement for small $k_2 r_2$, say, $k_2 r_2 < 0.3$. Also from Fig. 2, we see that the SCV approximation becomes progressively worse as $k_2 r_2$ approaches unity. This is expected as the SCV approximation requires that both $k_1 r_2$ and $k_2 r_2$ are much smaller than unity.

4. Energy conservation

In this section, we present a relationship between the rate at which the energy is extinguished by the cylindrical void from the $U^{(1)}(r,\theta)$ field. Also, a numerical example illustrating that the SCV approximation is in good agreement with the derived energy conservation relationship is presented.

We begin by constructing an imaginary concentric cylinder of radius $R>r_1$ and length L around the host cylinder shown in Fig. 1b. Then, the rate $\mathbb{W}_U^{(\mathrm{abs})}$ at which the energy is absorbed within the imaginary concentric cylinder is given by

$$\mathbb{W}_U^{(\mathrm{abs})} = -RL\int_{-\pi}^{\pi} \mathbf{S}_U\cdot\hat{\mathbf{r}}\,\mathrm{d}\theta, \tag{17a}$$

where $\hat{\mathbf{r}}=\cos\theta\,\hat{\mathbf{x}}+\sin\theta\,\hat{\mathbf{y}}$ (see Fig. 1), and the time-averaged Poynting vector is given by

$$\mathbf{S}_U = \frac{1}{2}\mathrm{Re}\left[\frac{\mathrm{i}c}{4\pi k}U^{(1)}\nabla\left(U^{(1)}\right)^*\right]. \tag{17b}$$

In (17b), Re denotes the real part, * denotes the complex conjugate, and $k=\omega/c$. Now, we consider the rate $\mathbb{W}_V^{(\mathrm{abs})}$ at which the energy is absorbed by the *cylindrical annulus*. By proceeding as before, we immediately obtain

$$\mathbb{W}_V^{(\mathrm{abs})} = -RL\int_{-\pi}^{\pi}\mathbf{S}_V\cdot\hat{\mathbf{r}}\,\mathrm{d}\theta,\quad \text{where } \mathbf{S}_V=\frac{1}{2}\mathrm{Re}\left[\frac{\mathrm{i}c}{4\pi k}V^{(1)}\nabla(V^{(1)})^*\right]. \tag{18}$$

Substituting $V^{(1)}=U^{(1)}+W^{(\mathrm{sca})}$ into (18) and using (17) to simplify the result yields

$$\mathbb{W}^{\mathrm{ext}} = \mathbb{W}_V^{(\mathrm{abs})}-\mathbb{W}_U^{(\mathrm{abs})}+\mathbb{W}_W^{(\mathrm{sca})}, \tag{19a}$$

where

$$\mathbb{W}^{\mathrm{ext}} = -\frac{RLc}{8\pi k}\int_{-\pi}^{\pi}\mathrm{Re}\left[\mathrm{i}U^{(1)}\nabla\left(W^{(\mathrm{sca})}\right)^*+\mathrm{i}W^{(\mathrm{sca})}\nabla\left(U^{(1)}\right)^*\right]\cdot\hat{\mathbf{r}}\,\mathrm{d}\theta \tag{19b}$$

and

$$\mathbb{W}_W^{(\mathrm{sca})} = \frac{RLc}{8\pi k}\int_{-\pi}^{\pi}\mathrm{Re}\left[\mathrm{i}W^{(\mathrm{sca})}\nabla\left(W^{(\mathrm{sca})}\right)^*\right]\cdot\hat{\mathbf{r}}\,\mathrm{d}\theta. \tag{19c}$$

We interpret $\mathbb{W}^{\mathrm{ext}}$ as the rate at which the energy is extinguished by a scatterer, namely, the cylindrical void, in the presence of the host cylinder. In other words, it is the rate at which the energy is depleted by the cylindrical void from the total field, $U^{(1)}$, outside the host cylinder. Moreover, from (19) we see that if the cylindrical annulus is nonabsorbing (ϵ_2 is purely real), then $\mathbb{W}^{\mathrm{ext}}=\mathbb{W}_W^{(\mathrm{sca})}$. Finally, substituting $U^{(1)}(r,\theta)$ and $W^{(\mathrm{sca})}(r,\theta)$ (see (9a) and (10)) into (19b), and then integrating the result over θ yields

$$\mathbb{W}^{\mathrm{ext}} = -\frac{Lc}{2\pi k}\sum_{n=0}^{\infty}g_n\left(\mathrm{Re}\left[A_n^{(\mathrm{cv})}\right]+2\mathrm{Re}\left[A_n^{(\mathrm{cv})}\left(A_n^{(\mathrm{hc})}\right)^*\right]\right). \tag{20}$$

We interpret the first term in (20) as the rate at which $W^{(\mathrm{sca})}$ extinguishes energy from $U^{(\mathrm{inc})}$, and the second term as the rate at which $W^{(\mathrm{sca})}$ extinguishes energy from $U^{(\mathrm{sca})}$.

To illustrate that the SCV approximation is in good agreement with the energy conservation principle, we compute $\mathbb{W}^{\mathrm{ext}}$ using the exact and approximate $A_n^{(\mathrm{cv})}$ coefficients. Recall that the exact $A_n^{(\mathrm{cv})}$ coefficients are given by (13), and the approximate coefficients by (15).

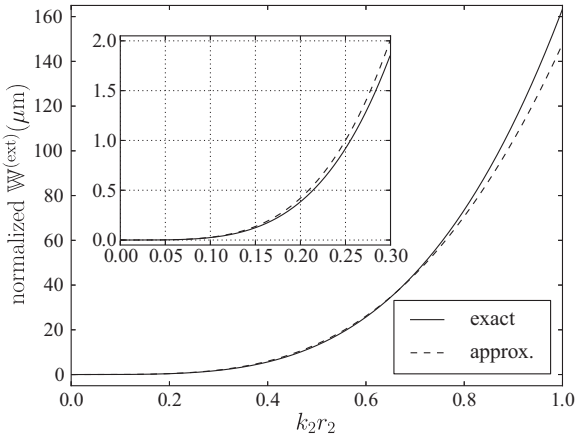

Fig. 3. The rate $\mathbb{W}^{\mathrm{ext}}$ (normalized by $Lc/8\pi$) at which energy is extinguished by the cylindrical void from the total field outside the host cylinder is shown as a function of k_2r_2. The above plot was produced with the same parameters as the ones described in the caption of Fig. 2.

The results of the above-mentioned computations are shown in Fig. 3. From Fig. 3, we see that the SCV approximation conserves energy to roughly 10% for $k_2r_2\le 1$, which does indicate that the SCV approximation is in good agreement with the energy conservation principle.

5. Conclusions

In this paper, we investigated a monochromatic plane wave scattering from a solid homogeneous cylinder (host cylinder) and a cylindrical annulus, referring to the inner part of the cylindrical annulus as the cylindrical void. It was shown that if the cylindrical void is thought of as a scatterer inserted into the host cylinder, then the scattered field due to the cylindrical void may be approximated by the screened cylindrical void (SCV) approximation, see Section 2. The SCV approximation was derived intuitively in Section 2 and rigorously in Section 3. Furthermore, a formula for the rate at which energy is depleted by the cylindrical void from the total field outside the host cylinder was derived in Section 4. The numerical examples in Sections 3 and 4 showed that the SCV approximation is in good agreement with the exact solution if the cylindrical void is small.

Acknowledgments

This material is based upon work supported in part by the U.S. Office of Naval Research as a Multi-disciplinary University Research Initiative on Sound and Electromagnetic Interacting Waves under grant number N00014-10-1-0958.

References

[1] Kerker M. The scattering of light and other electromagnetic radiation. New York: Academic Press; 1969.
[2] van de Hulst HC. Light scattering by small particles. New York: Dover; 1981.

[3] Bohren CF, Huffman DR. Absorption and scattering of light by small particles. New York: John Wiley & Sons; 1983.
[4] Gouesbet G. Generalized Lorenz–Mie theories, the third decade: a perspective. J Quant Spectrosc Radiat Transfer 2009;110:1223–38.
[5] Debye P. Das elektromagnetische feld um einen zylinder und die theorie des regenbogens. Phys Z 1908;9:775–8. (Reprinted and translated into English in P.L. Marston (Ed.), Geometrical Aspects of Scattering, volume MS89 of Milestone Series, SPIE, Bellingham, Wash., 1994, pp. 198–204.).
[6] Li R, Han X, Jiang H, Ren KF. Debye series of normally incident plane-wave scattering by an infinite multilayered cylinder. Appl Opt 2006;45:6255–62.
[7] Li R, Han X, Ren KF. Generalized Debye series expansion of electromagnetic plane wave scattering by an infinite multilayered cylinder at oblique incidence. Phys Rev E 2009;79:036602.
[8] Anderson PW. Absence of diffusion in certain random lattices. Phys Rev 1958;109:1492–505.
[9] Lagendijk A, van Tiggelen B, Wiersma DS. Fifty years of Anderson localization. Phys Today 2009;62:24–9.
[10] Scales JA, Carr LD, McIntosh DB, Freilikher V, Bliokh YP. Millimeter wave localization: slow light and enhanced absorption in random dielectric media. Phys Rev B 2007;76:085118.
[11] Rusek M, Orłowski A. Analytical approach to localization of electromagnetic waves in two-dimensional random media. Phys Rev E 1995;51:R2763–6.
[12] Rusek M, Orłowski A. Example of self-averaging in three dimensions: Anderson localization of electromagnetic waves in random distributions of pointlike scatterers. Phys Rev E 1997;56:6090–4.
[13] Abramowitz M, Stegun IA, editors. Handbook of mathematical functions. New York: Dover; 1965.